UMYU Scientifica, Vol. 2 NO. 3, September 2023, Pp 108 – 120
https://doi.org/10.56919/usci.2323.017
ISSN: 2955 – 1145 (print); 2955 – 1153 (online)
A periodical of the Faculty of Natural and Applied Sciences, UMYU, Katsina

ORIGINAL RESEARCH ARTICLE

Influence of Soret and Radial Magnetic Field on Natural Convection of a Chemically Reactive Fluid in an Upright Porous Annulus.

Godwin Ojemeri[1]*, Muhammed Murtala Hamza[2], Badamasi Haliru Tambuwal[3], Ibrahim Bello[4] and Abdulsalam Shuaibu[5].

[1,5]Department of Mathematics, College of Sciences, Federal University of Agriculture, P. M. B. 28, Zuru, Kebbi State, Nigeria.
[2]Department of Mathematics, Faculty of Physical and Computing Sciences, Usmanu Danfodiyo University, P. M. B. 2346, Sokoto, Nigeria.
[3]Department of Mathematics, Shehu Shagari College of Education, P. M. B. 2129, Sokoto.
[4]Department of Medical X-ray Technician, Sultan Abdulraham School of Health Technology, P. M. B. 1006, Gwadabawa, Sokoto, Nigeria.

ABSTRACT

Mass fluxes produced by temperature gradients is known as the Soret or thermal-diffusion effect and this effect can be very crucial in the appearance of strong density difference in the flow premises. This article therefore explores the analytical solutions of natural convection of a chemical reacting fluid in the involvement of Soret and radial magnetic field in an annular upstanding permeable zone within concentric cylinders' r = 1 and r = b. The non-linear formulated equations that govern the flow are resolved by a semi-analytical approach. The consequences of the numerous governing controlling parameters embedded in the formulated model is thoroughly described with the use of illustrative plots. It is noteworthy to report that raising the levels of Frank–Kamenetskii, sustentation, and thermo-diffusion parameters increases fluid velocity whereas reducing the radial magnetic field effect weakens the fluid flow. Additionally, it is significant to report that the sheer stress on the annular walls can be effectively regulated by applying appropriate values of magnetic number. In conclusion, the variations of the key parameters in this study can be used more effectively to control heat transfer and fluid flow using an annular geometry. This study can find relevance in geothermal power generation, drilling activities, space vehicles technology and nuclear power plants etc.

ARTICLE HISTORY

Received June 29, 2023.
Accepted September 18, 2023.
Published September 30, 2023.

KEYWORDS

Natural convection, Chemically reactive fluid, Soret effect, Radial magnetic field, Vertical permeable annulus, Semi-analytical approach.

INTRODUCTION

Researching the implications of heat and mass transfer across a chemically reacting fluids enclosed by various geometrical shapes is of particular interest to researchers attributed to its relevance to transpiration cooling of re-entry vehicles, rocket boosters and film vaporization in combustion chambers (Muthuraj and Srinivas, 2010). The simulation of chemical reacting fluids was first proposed by Frank Kamenetskii in 1969. As asserted by (Makinde 2008), most of lubricants utilized in industrial and technological operations, namely synthetic esters, polyphony lathers, hydrocarbon oils, polyglycols, and so forth, are reactive. With these concerns in mind, works of Hamza *et al.* (2023a, 2023b) recently shed more light on the implications of hydromagnetic natural convection of a chemically reacting fluid using homotopy perturbation technique. It is concluded from their results that mounting level of Frank-Kamenetskii, representing the viscous heating term is noticed to encourage both the thermal and hydromagnetic fluid. Ojemeri and Onwubuya (2023) describe the analysis of steady mixed convection flow of Arrhenius-controlled chemical reaction and an exothermic fluid along an isothermally heated superhydrophobic microchannel due to heat source/sink. Ojemeri *et al.* (2023) focused their search on the analytical treatment of Arrhenius-controlled fluid in an upright microchannel saturated with porous material using homotopy perturbation method (HPM) restricted to an appropriate boundary conditions. Their results showed that the variations of chemical reaction, Darcy number, rarefaction and wall-ambient temperature parameters substantially dictate the fluid flow and volume flow rate respectively. Ojemeri and Hamza (2022) put forth a computational treatment of an Arrhenius kinetically propelled heat emission and absorption fluid in a microchannel. Ahmad and Jha (2015) conducted a numerical and an analytical investigations of the influence of heat transfer flow of an

Correspondence: Godwin Ojemeri. Department of Mathematics, Faculty of Sciences, Federal University of Agriculture, P. M. B. 28, Zuru, Kebbi State, Nigeria. ✉ godwinojemeri@gmail.com. Phone Number: +234 806 167 6148.
How to cite: Ojemeri, G., Hamza, M. M., Tambuwal, B. H., Bello, I., & Shuaibu, A. (2023). Influence of Soret and Radial Magnetic Field on Natural Convection of a Chemically Reactive Fluid in an Upright Porous Annulus. *UMYU Scientifica*, 2(3), 108 – 120. https://doi.org/10.56919/usci.2323.017

exothermic chemical reacting fluids in an upstanding porous pipe. Their findings depict that heat transmission amount on pipe surfaces, whether transient or steady-state, increases with time. Jha *et al.* (2011a, 2011b) studied the time-dependent natural convection of an exothermic reaction fluid in an upright channel restricted to two immeasurable upright parallel plates as well as in a tube. They concluded that the amount of heat transmission and sheer stress on both walls increases as the chemical reactant parameter is increased. References like Ojemeri *et al.* (2019), Hamza *et al.* (2019), Ali *et al.* (2014), Hamza (2016) shed more light on this phenomenon

As a result of recent scientific and technological achievements, annular space applications in industry and engineering have continued to gain a lot of attention. The fields of heat exchangers and oil and gas well drilling operations (Jha *et al.* 2015) provide such examples. Related studies on natural convection flows in an upstanding annulus can be found in other literature. Joshi (1987) modeled natural convection flow in upstanding annuli having two isothermal limits, one warmer than the other. The thermo-diffusion effect is the diffusion of mass as a result of a temperature gradient, and it can be significant when the flow region has large density differences. Further, this impact can be considerable when species are applied at the surface of a fluid region with a density less than the nearby fluid. The thermal diffusion factor has been used to separate isotopes as well as to combine gases with very light and medium molecular weights (Sravanthi 2014). Ahmad *et al.* (2017) studied the steady state mixed convective heat and mass transfer flow of an exothermic chemically reacting fluid in an upward porous conduit affected by Soret effect. According to their findings, the Soret effect and mixed convection had a remarkable impact on the fluid velocity in the pipe. Kaladhar *et al.* (2016) examined the radiation and thermal diffusion actions on mixed convection of a pair stress fluid between two permeable vertical plates. Srinivasacharya and Kaladhar (2013) inspected the thermos-diffusion and Dufour actions on the natural convection of a couple fluids in an upright channel with chemical interaction. In a separate study, Srinivasacharya and Kaladhar (2014) studied the chemical reactions, Soret, and Dufour factors on mixed convection flow between vertical parallel plates of a pair stress fluid. Cheng (2009) examined the thermal diffusion and Dufour impacts on natural convective heat and mass transport through a porous upstanding plate.

Investigators have in recent times beamed their searchlight on the analysis of magneto-hydrodynamics (MHD) due to its numerous possible implications it could have in astronomy, geophysics, and engineering. These assessments are essential in a number of industries, such as space vehicle technology, extraction processes, nuclear power facilities, and geothermal power generation. (Vanita and Kumar 2016). Globe (1959) was the first to present the annular MHD flow problem, concentrating on steady laminar hydromagnetic flow in an annular channel. Quite recently, Yale *et al.* (2023) investigated the impact of MHD free convection of an incompressible fluid in the presence of viscous dissipation through a heated superhydrophobic microchannel. They concluded that the actions of viscous dissipation and super-hydrophobicity is seen to significantly encourage the fluid flow. Taid and Ahmed (2022) applied the perturbation technique to determine the consequences of the thermal diffusion, viscous dissipation, and chemical reaction on steady two-dimensional MHD free flow along an inclined permeable channel entrenched in a porous material. Osman *et al.* (2022) discussed the action of MHD on natural convection flow along an immeasurable inclined plate using the Laplace transformation approach. Siva *et al.* (2021) echoed the significance of hydromagnetic action on a heat transfer problem of electrokinetic flow in a rotational microfluidic channel. Mozayyeni and Rahimi (2012) investigated mixed convection in an upright annulus in the involvement of a radial magnetic field and they concluded that using an external magnetic field can successfully reduce fluid velocity and temperature. Reddy and Reddy (2009) studied the effects of radiation and mass transfer on the time-dependent hydromagnetic flow of an electrically-conducting fluid across a moving upright cylinder. They analyzed the flow patterns of momentum, energy, mass diffusion, drag force and rates of heat and mass transfers based on the fluctuations in the regulating thermo-physical and hydro-dynamical factors. Other works published to exemplify this concept include Ali *et al.* (2013), Javaherdeh *et al.* (2015), Sankar *et al.* (2006), to cite a few.

The purpose of this article is to basically modify the work conducted by Ahmad *et al.* (2017) by carrying out a steady state investigation of thermal diffusion and radial magnetic field effects on the free convection of a viscous reactive fluid in an upstanding porous annulus. The novelty of this work is in the fact that a different flow geometry was considered, ie, the porous annulus, which is a more effective tool for controlling heat transfer and fluid flow in both tall and shallow cavities. Moreover, the annulus model is a more general flow channel than the cylindrical pipe used in the the previous literature. When $\lambda \to \infty$, the annulus approaches a cylindrical pipe whereas when $\lambda \to 1$, the annulus behaves like two parallel plates. When the value of λ is in between, the curvature differences between the inner and outer walls can lead to various flow patterns. The formulated model is a set of nonlinear ordinary differential equations in terms of mass diffusion, energy and momentum, which has been solved semi-analytically by a regular perturbation approach with a power series expansion in the reactant consumption parameter λ. Shear stress, heat and mass transfer rates have also been calculated. Major parameters controlling the different flow patterns are graphically presented and discussed. The results of this investigation can find relevance in areas such as lubrication industries, chemical engineering, biomedical sciences, processing and drilling industries, and so forth.

MATERIALS AND METHODS

Mathematical Analysis

Figure 1 depicts the geometry of the current paper under discussion in schematic form. As illustrated in figure 1, we investigate a steady state free convection of chemically reacting fluid with soret and a radial magnetic number in an upright permeable annulus of unlimited length. The fluid is thought to be Newtonian and obeys Boussinesq's approximation when immersed in it at a constant temperature T_0. Following Ahmad *et al.* (2017) and Hamza *et al.* (2019), the dimensional form of the diffusion, temperature, and velocity equations under the aforementioned assumptions are:

$$\frac{\partial u'}{\partial t'}+\frac{v_0 b}{r'}\frac{\partial u'}{\partial r'}=\nu\left[\frac{\partial^2 u'}{\partial r'^2}+\frac{1}{r'}\frac{\partial u'}{\partial r'}\right]+g\beta\left(T'-T_0\right)+g\beta^*\left(\phi'-\phi_0\right)-\frac{\sigma\beta_0^2 b^*}{\rho r'}u' \tag{1}$$

$$\frac{\partial T'}{\partial t'}+\frac{v_0 b}{r'}\frac{\partial T'}{\partial r'}=\alpha\left[\frac{\partial^2 T'}{\partial r'^2}+\frac{1}{r'}\frac{\partial T'}{\partial r'}\right]+\frac{QC_0 A}{\rho C_p}\exp\left(-\frac{E}{RT'}\right) \tag{2}$$

$$\frac{\partial \phi'}{\partial t'}+\frac{v_0 b}{r'}\frac{\partial \phi'}{\partial r'}=D_m\left[\frac{\partial^2 \phi'}{\partial r'^2}+\frac{1}{r'}\frac{\partial \phi'}{\partial r'}\right]+\frac{D_m K_T}{T_m}\left[\frac{\partial^2 T'}{\partial r'^2}+\frac{1}{r'}\frac{\partial T'}{\partial r'}\right] \tag{3}$$

The initial and boundary conditions to be satisfied are:

$$\left.\begin{array}{l} u'=0,\theta'=\theta_0,\phi'=\phi_0 for a^*\le r'\le b^* \\ \{u'=0,T'=T_w',\phi'=\phi_w' at r'=a^* \\ u'=0\theta'=0\phi'=0 at r'=b^* \end{array}\right\} \tag{4}$$

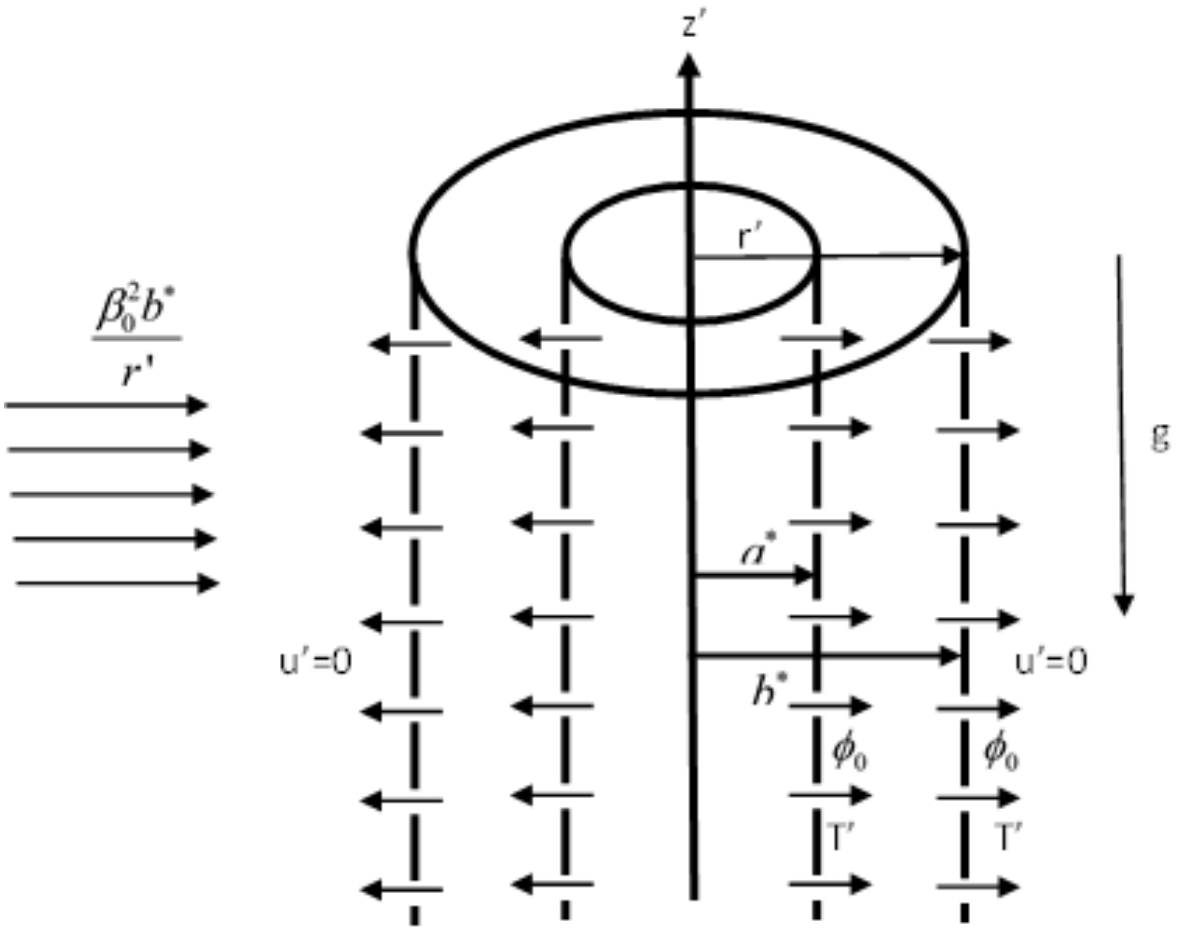

Fig. 1 Physical coordinate of the flow domain

we introduce the non-dimensional quantities:

$$u=\frac{u'}{U_0},t=\frac{t'\nu}{b^2},\theta=\frac{E}{RT_0^2}\left(T'-T_0\right),\phi=\frac{E\left(\phi'-\phi_0\right)}{R\phi_0^2},\lambda=\frac{QC_0AEb^2}{kRT_0^2}\exp\left(-\frac{E}{RT_0}\right),Sc=\frac{\nu}{D},$$

$$Sr=\frac{D_mK_T\left(T_1-T_0\right)}{\nu T_1\left(C_1-C_0\right)},N=\frac{\beta^*\left(\phi_1-\phi_0\right)}{\beta\left(T_1-T_0\right)},M^2=\frac{\sigma B_0^2r_0^2}{\rho\nu},b=\frac{b^*}{a^*},\theta_a=\frac{E\left(T_w-T_0\right)}{RT_0^2}$$

$$\varepsilon=\frac{RT_0}{E},r=\frac{r'}{b},s=\frac{v_0b}{\nu},\phi_a=\frac{E\left(\phi_w-\phi_0\right)}{R\phi_0^2} \tag{5}$$

Analytical Solutions

The steady state solutions for the reactive viscous fluid's concentration, temperature, and velocity fields, as well as sheer stress, rates of heat and mass transfers, are obtained. When non-dimensional quantities are introduced, the closed-form resultant governing equations of this model become:

$$\frac{d^2u}{dr^2}+\frac{1}{r}\left(1-s\right)\frac{du}{dr}-\frac{M^2U}{r^2}+\theta+N\phi=0 \tag{6}$$

$$\frac{d^2\theta}{dr^2}+\frac{1}{r}\left(1-s\,\mathrm{Pr}\right)\frac{d\theta}{dr}+\lambda\exp\left(\frac{\theta}{1+\varepsilon\theta}\right)=0 \tag{7}$$

$$\frac{d^2\phi}{dr^2}+\frac{1}{r}\left(1-sSc\right)\frac{d\phi}{dr}=-Sr\left[\frac{d^2\theta}{dr^2}+\frac{1}{r}\frac{d\theta}{dr}\right] \tag{8}$$

Restricted to the boundary conditions below:

$$\begin{aligned}&u=0,\quad\theta=\theta_a,\phi=\phi_a\quad at\qquad r=1\\&u=0,\quad\theta=0,\quad\phi=0\quad at\qquad r=b\end{aligned} \tag{9}$$

Where M, s, Pr, Sc, Sr, λ, ε, θ_a, and ϕ_a are magnetic field, suction/injection, Prandlt number, Schmidt number, Soret number, chemical reacting parameter, activation energy, ambient temperature and ambient concentration parameters respectively.

Because the problem is extremely nonlinear, we used a regular perturbation technique with a power series expansion in the reactant consumption parameter λ.

$$\phi=\phi_0+\lambda\phi_1+\lambda^2\phi_2+\lambda^3\phi_3+0(\lambda) \tag{10}$$

$$\theta=\theta_0+\lambda\theta_1+\lambda^2\theta_2+\lambda^3\theta_3+0(\lambda) \tag{11}$$

$$U=u_0+\lambda u_1+\lambda^2u_2+\lambda^3u_3+0(\lambda) \tag{12}$$

inserting egns (10) and (11) and (12) into eqns (6), (7) and (8) and comparing the coefficients of like powers of λ,the analytical solutions for the governing equations are obtained as follows:

$$U = \lambda\left[A_3 r^{z1} + A_4 r^{-z2} + B_3 r^2\right] + \lambda^2\left[A_5 r^{z1} + A_6 r^{-z2} + B_7 r^4 + B_8 r^3 + B_9 r^2\right] + \lambda^3\left[A_7 r^{z1} + A_8 r^{-z2} + B_{13} r^6 + B_{14} r^5 + B_{15} r^4 + B_{16} r^3 + B_{17} r^2\right] \quad (13)$$

$$\theta = x_4\left(k_1 r + k_2\right) + \lambda\left[x_2\left(2k_3 r + 2k_4 - r^2\right)\right] + \lambda^2\left[x_4 x_2\left(\frac{r^4}{12} - \frac{k_3 r^3}{3} - k_4 r^2\right) + x_4\left(k_5 r + k_6\right)\right] + \lambda^3\left[\left\{x_4^2 x_2\left(\frac{k_4 r^4}{12} + \frac{k_3 r^5}{60} - \frac{r^6}{360}\right) - x_4^2\left(\frac{k_5 r^3}{6} + \frac{k_6 r^2}{2}\right)\right\} + x_1 x_3 x_4\left(\frac{r^6}{30} - \frac{k_3 r^5}{5} - \frac{k_4 r^4}{3} + \left(\frac{k_3^2 r^4}{3} + \frac{4k_3 k_4 r^3}{3} + 2k_4^2 r^2\right) + x_4\left(k_7 r + k_8\right)\right]\right] \quad (14)$$

$$\phi = -x_5 Sr\left(x_4 k_1\left(rIn(r) - r\right)\right) + x_5\left(k_9 r + k_{10}\right) + \lambda\left[-x_5 Sr\left(2x_2 k_3\left(rIn(r) - r\right) - 2x_2 r^2\right) + x_5\left(k_{11} r + k_{12}\right)\right] + \lambda^2\left[-x_5 Sr\left\{x_4 x_2\left(\frac{r^4}{9} - \frac{k_3 r^3}{2} - 2k_4 r^2\right) + x_4 k_5\left(rIn(r) - r\right)\right\} + x_5\left(k_{13} r + k_{14}\right)\right] + \lambda^3\left[-x_5 Sr\left\{x_4^2 x_2\left(\frac{k_4 r^4}{9} + \frac{k_3 r^5}{48} - \frac{r^6}{300}\right) - x_4^2\left(\frac{k_5 r^3}{4} + k_6 r^2\right)\right\} + x_1 x_3 x_4\left(\frac{r^6}{25} - \frac{k_3 r^5}{4} - \frac{4k_4 r^4}{9} + \frac{4k_3^2 r^4}{9} + 2k_3 k_4 r^3 + 4k_4^2 r^2\right) + x_4 k_7\left(rIn(r) - r\right)\right\} + x_5\left(k_{15} r + k_{16}\right)\right] \quad (15)$$

The skin frictions on the boundaries are:

$$\tau_1 = \left.\frac{dU}{dr}\right|_{r=1} = \lambda\left(z1A_3 - z2A_4 + 2B_3\right) + \lambda^2\left(z1A_5 - z2A_6 + 4B_6 + 3B_7 + 2B_8\right) + \lambda^3\left(z1A_7 - z2A_8 + 6B_{11} + 5B_{12} + 4B_{13} + 3B_{14} + 2B_{15}\right) \quad (16)$$

$$\tau_b = \left.\frac{dU}{dr}\right|_{r=b} = \lambda\left(z1A_3 b^{z1-1} - z2A_4 b^{-z2-1} + 2B_3 b\right) + \lambda^2\left(z1A_5 b^{z1-1} - z2A_6 b^{-z2-1} + 4B_6 b^3 + 3B_7 b^2 + 2B_8 b\right) + \lambda^3\left(z1A_7 b^{z1-1} - z2A_8 b^{-z2-1} + 6B_{11} b^5 + 5B_{12} b^4 + 4B_{13} b^3 + 3B_{14} b^2 + 2B_{15} b\right) \quad (17)$$

The mass and heat transfer on both boundaries is equal, attributable to the uniform nature of the flow, and as a result, the steady-state rates of heat and mass transfers on the boundaries are derived as follows:

$$Nu = \left.\frac{d\theta}{dr}\right|_{r=b} = x_4 k_1 + \lambda\left[2x_2\left(k_3 - b\right)\right] + \lambda^2\left[x_4 x_2\left(\frac{b^3}{3} - k_3 b^2 - 2k_4 b\right) + x_4 k_5\right] + \lambda^3\left[x_4^2 x_2\left(\frac{k_4 b^3}{3} + \frac{k_3 b^4}{12} - \frac{b^5}{60}\right) - x_4^2\left(\frac{k_5 b^2}{2} + k_6 b\right) + x_1 x_3 x_4\left(\frac{b^5}{5} - k_3 r^4 - \frac{4k_4 b^4}{3} + \frac{4k_3^2 b^3}{3} - 4k_3 k_4 b^2 + 4k_4^2 b\right) + x_4 k_7\right] \quad (18)$$

$$Sh = \left.\frac{d\phi}{dr}\right|_{r=b} = \left[-x_5x_4k_1Sr\left(In(b)\right)\right] + x_5k_9 + \lambda\left[-x_5Sr\left(2x_2k_3In(b) - 4x_2\right) + x_5k_{11}\right] +$$
$$\lambda^2\left[-x_5Sr\left\{x_4x_2\left(\frac{4b^3}{9} - \frac{3k_3b^2}{2} - 4k_4b\right) + x_4k_5In(b)\right\} + x_5k_{13}\right] + \lambda^3\left[x_5Sr\left\{x_4^2x_2\left(\frac{4k_4b^3}{9} - \frac{5k_3b^4}{48}\right.\right.\right.$$
$$\left.\left.\left. - \frac{b^5}{50}\right) - x_5Sr\left(\frac{3k_5b^2}{4} + 2k_6b\right) + x_1x_3x_4\left(\frac{6b^5}{25} - \frac{5k_3b^4}{4} - \frac{16k_4b^3}{9} + \frac{16k_3^2b^3}{9} + 6k_3k_4b^2 + 8k_4^2b\right)\right.\right.$$
$$\left.\left. + x_4k_7In(b)\right\} + x_5k_{15}\right] \qquad (19)$$

where $x_1, x_2, x_3, x_4, x_5, k_1, k_2, k_3, k_4, k_5, k_6k_7, k_8, k_9, k_{10}, k_{11}, k_{12}, k_{13}, k_{14}, k_{15}, k_{16}, A_3, A_4, A_5$

$A_6, A_7, A_8, B_3, B_7, B_8, B_9, B_{13}, B_{14}, B_{15}, B_{16}, B_{17}$ *are indicated* in *the appendix.*

RESULTS AND DISCUSSION

The natural convection of a hydromagnetic chemical reacting fluids with Soret and radial magnetic field effects is investigated in an upright permeable annulus. The We have shown the impacts of petinent parameters like Frank-Kamenetskii (λ), Sustentation (N), Soret number (Sr), and magnetic number (M) on the flow configurations in Fig. 2-15, using the default values of λ=0.001, Sr=1, Sc=0.22, ε=0.01, Pr=0.71, s=3, θ_a=1, ϕ_a=1.

The influence of λ on temperature, concentration, and velocity distributions are depicted in Figures 2-4. These graphs show that as λ grows the temperature, concentration, and velocity of the fluid grow. This is owing to the truth that a growth in λ, which basically denotes the viscous heating parameter, corresponds to an increase in the chemical reaction's strength. Naturally speaking, these results make sense, as raising the heat source parameter indicates more heat generation from the region's surface, making the fluid to accelerate faster, thereby resulting in high performance of the system. There are many thermal applications where this result can find relevance which include power generation, space heating, cooking and industrial processes, to mention a few. These results corroborate with those obtained by Obalalu *et al.* (2021) and Hamza (2016). The actions of Soret on concentration and velocity gradients can be seen in Figures 5 and 6. As can be seen from these graphs, increasing the value of Sr increases the fluid's concentration and velocity. This is physically true because the effect of Soret number appears in suspended mixture of particles and fluid and this phenomenon is made available by temperature gradients, consequently, the transport of fluid molecule in the highest energy level moves the particles to coldest region. This concept is very applicable in chemical and petroleum engineering processes as asserted by Ahammad and Krishna (2021). The effect of Sc on concentration is shown in Fig. 7, and it is clear that as the Schmidlt number increases, the mass flux decreases. Figures 8–10 show the impacts of Pr, M, and N on the fluid flow. As illustrated in these graphs, increasing the Pr and M parameters decreases fluid flow. The fact that M = 0 implies that the flow is totally hydrodynamic and that there is no magnetic effect. As the value of M grows, the velocity drops, as demonstrated in this diagram. This is to be expected, as the Lorentz force, which is a resistance-type force, is always produced when a transverse magnetic field is introduced. When M grows, the drag force tends to resist the fluid motion, leading to a considerable reduction in fluid speed. On the other hand, increases in N boost up the velocity of the flow, which also coincide with the findings of Hamza *et al.* (2019).

Figures 11-14 show the effects of varying frictional factor levels at the isothermal boundary at r = 1 (at the external wall of the inner cylinder) and r = b (at the inner surface of the outer cylinder). Figure 11 depicts the effect of λ and Sr on the sheer stress. At r = 1, increasing λ and Sr strengthens the drag force, but at r = b, increasing λ and Sr decreases the drag force as portrayed in (Figure 11b). Raising the levels of both λ and M reduces the sheer stress for r = 1, as shown in Figure 12a, but for r = b, the opposite occurs, as shown in Figure 12b. Figure 13 depicts the impacts of λ and Pr on the frictional factors. When r = 1, increasing the Prandlt number causes skin friction to increase, whereas increasing the value of λ causes skin friction to decrease. Figure 13b shows the opposite at r = b. Figure 14a shows that skin friction increases as both λ and N climb. When r = b, however, as illustrated in Figure 14b, the opposite is true. The influence of Sr and Pr on Nusselt number and Sherwood number, respectively, against λ is depicted in Figure 15. Raising the value of Pr reduces the rate of heat transmission, whereas increasing the value of λ increases the rate of heat transfer, as illustrated in Figure 15a. Physically, as λ rises, the fluid temperature rises with it, as does the temperature gradient, resulting in a faster heat transfer rate. The influence of λ and Sr on the mass transfer rate is depicted in Figure 15b. As indicated in the figure, increasing both λ and Sr yealds a larger mass transfer flow.

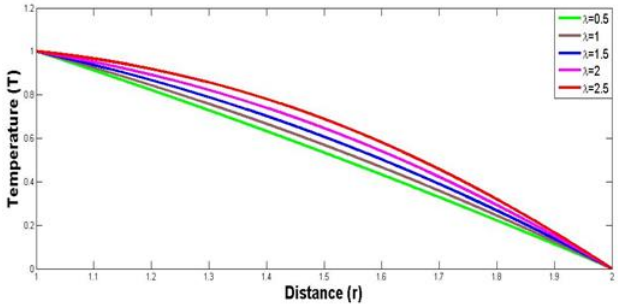

Figure 2λon temperature profile

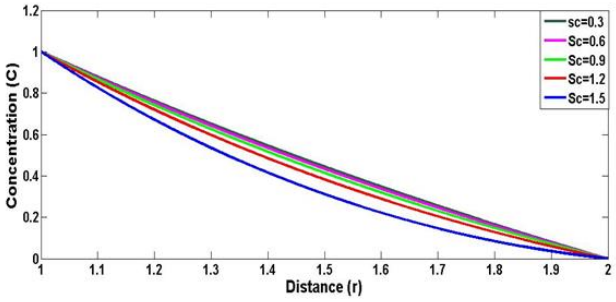

Figure 7 Sc on Concentration profile

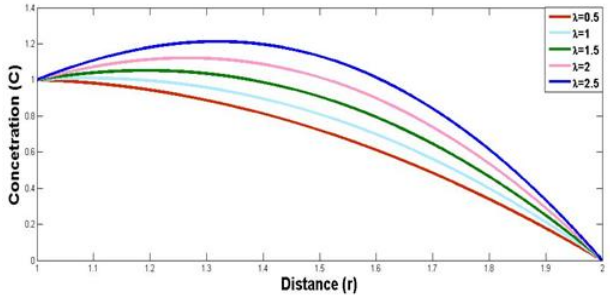

Figure 3 λon Concentration profile

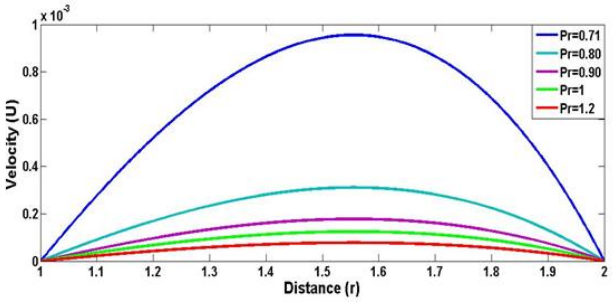

Figure 8 Pr on Velocity profile

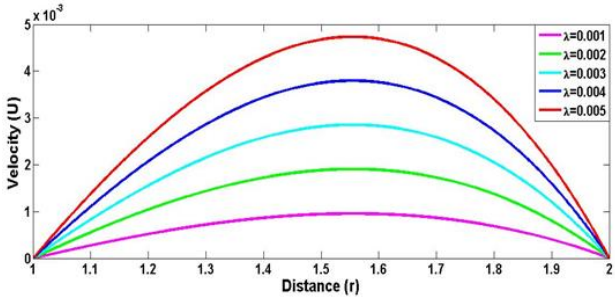

Figure 4 λon Velocity profile

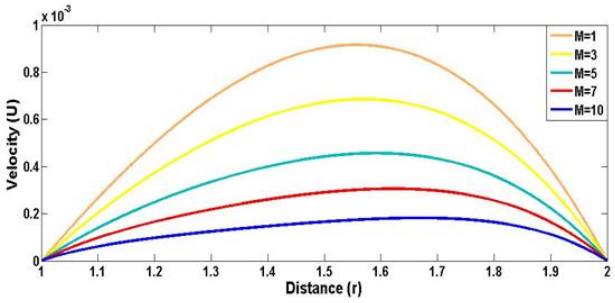

Figure 9 M on Velocity profile

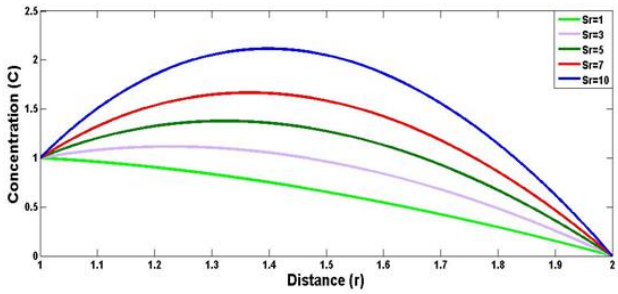

Figure 5 Sr on Concentration profile

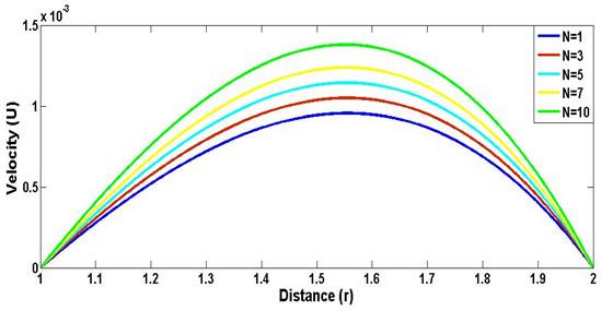

Figure 10 N on Velocity profile

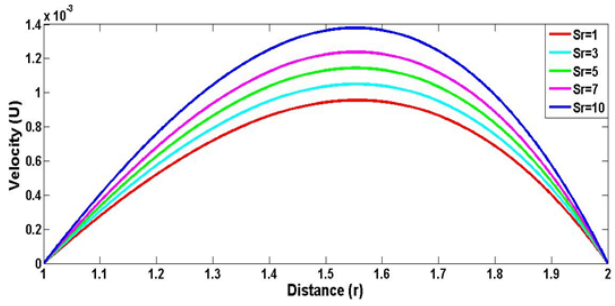

Figure 6 Sr on Velocity profile

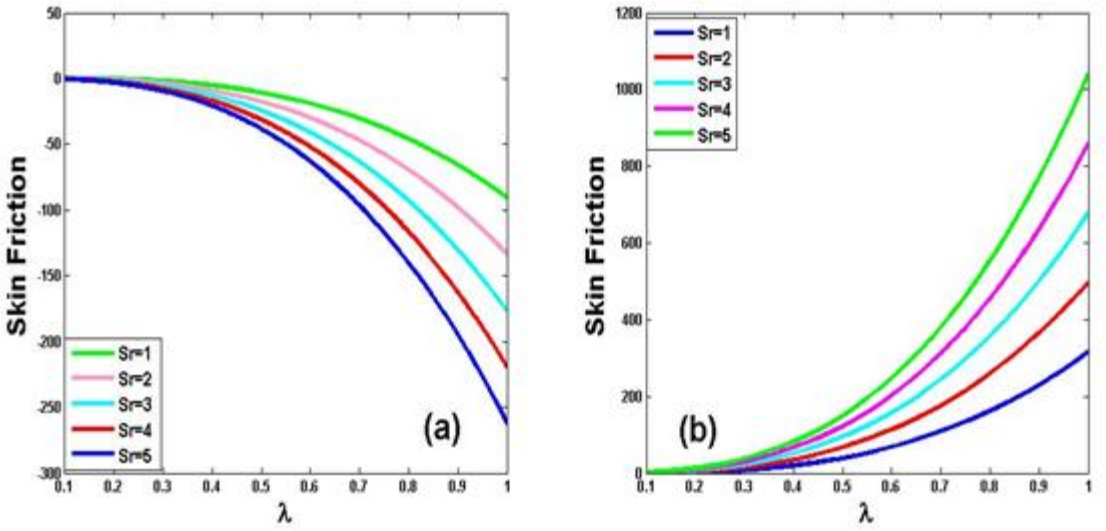

Figure 11 Sr on Skin friction

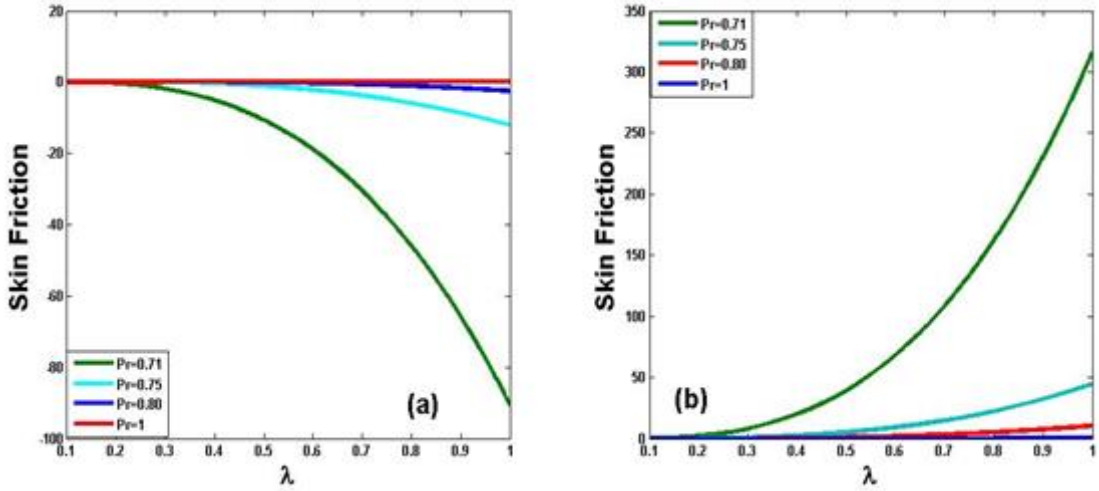

Figure 12 Pr on Skin friction

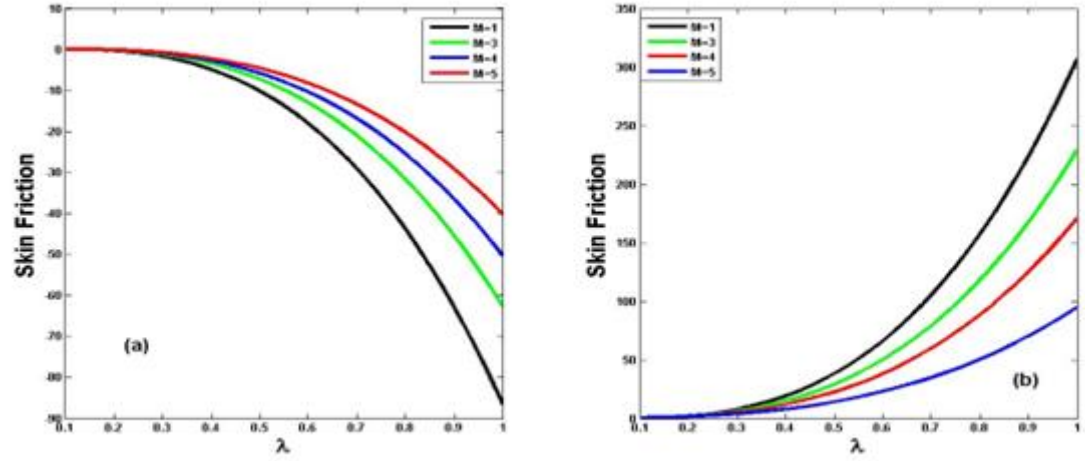

Figure 13 M on Skin friction

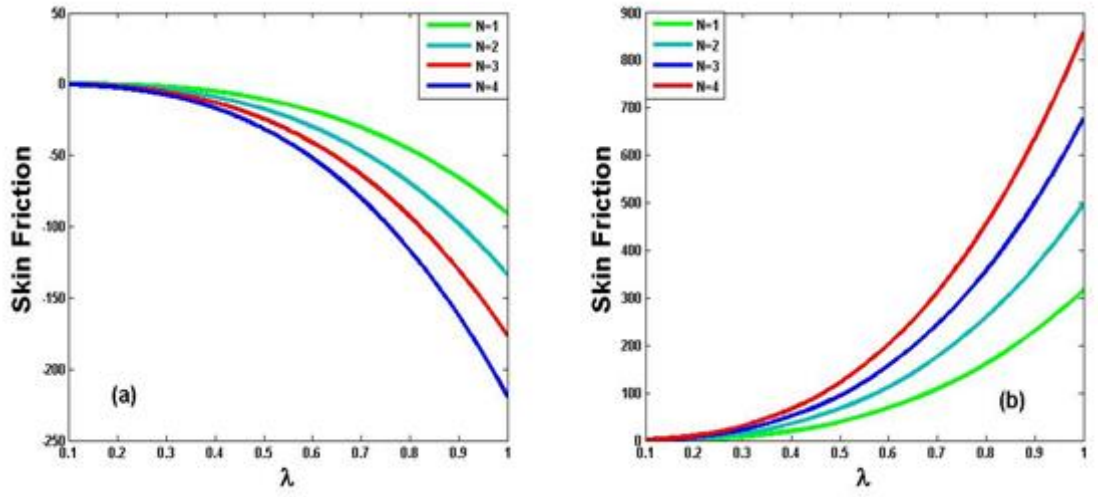

Figure 14 N on Skin friction

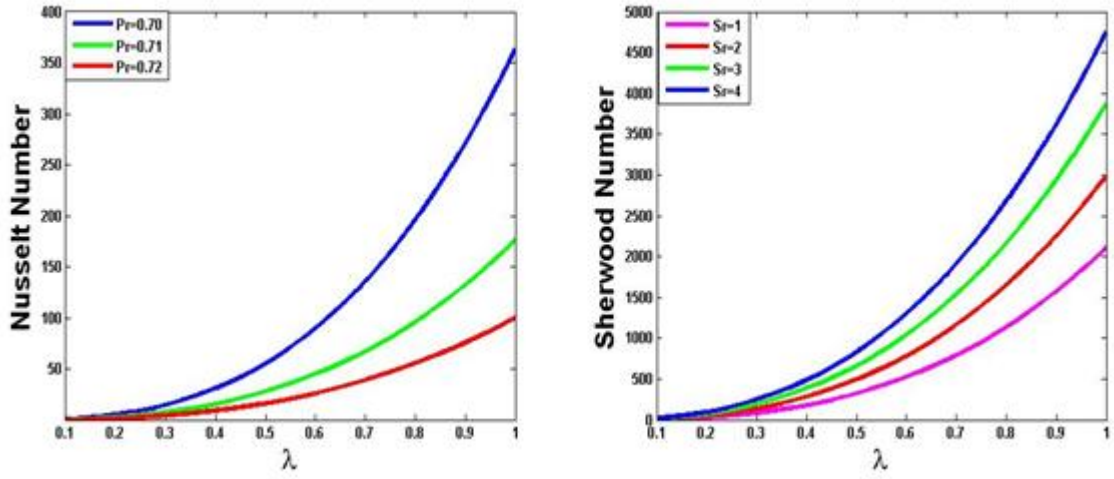

Figure 15 Pr and Sr against λ on Nusselt number and Sherwood number

CONCLUSIONS

In this study, we analyze the steady-state hydromagnetic flows for mass diffusion, temperature, momentum, shear stress, Nusselt, and Sherwood numbers in an upright permeable annulus for chemical reacting fluids affected by Soret and radial magnetic field impacts. Using a perturbation series technique, we determine the nonlinear steady state governing equations analytically. We examine the impacts of Frank-Kamenetskii (λ), sustentation (N), thermos-diffusion (Sr), and radial magnetic field (M) on flow configuration. Our findings suggest that increasing the values of Frank–Kamenetskii, sustentation, and thermal diffusion parameters improves the speed of the fluid, while higher values of radial magnetic field slow down the fluid flow. Furthermore, we observe that stronger temperature and concentration gradients lead to increased amounts of heat and mass transfer flow, respectively. The outcomes of this research correspond to those found in previously published results such as that of Ahmad *et al.* (2017) and Hamza *et al.* (2019). In practical situations, the annular geometry is a more useful mechanism for heat exchangers, which is typically used for gas cooled nuclear reactors as well as in drilling activities of oil and gas wells. Also, the Soret effect has been used as a means of isotope separation and in a mixture of gases of very light and medium molecular weights. In the future, this study can be expanded to investigate the effect of time as well as the action of chemical reaction.

REFERENCES

Ahammad N. A. and Krishna M. V (2021). Numerical Investigation of Chemical Reaction, Soret and Dufour Impacts on MHD Free Convective Gyrating Flow through a Vertical Porous Channel, Case Studies in Thermal Engineering, 28, 101571, **[Crossref]**.

Ahmad K. S and Jha B. K (2015). Computational Methods of Transient/steady Natural Convection Flow of Reactive Viscous Fluid in Vertical Porous Pipe. *Asian Journal of Mathematics and Computer Research*.2, 74-92.

Ahmad S. K., Ojemeri G. and Hamza M. M. (2017). Mixed Convective Heat and Mass Transfer Flow of Reactive Viscous Fluid in a Vertical Porous Pipe in the Presence of Thermal Diffusion, *Asian journal of mathematics and computer research*, 17, 73-87.

Ali, F., Khan, I. Shafie, S. S. (2013). Conjugate Effect of Heat and Mass Transfer on MHD Free Convection Flow over an Inclined Plate Embedded in Porous Medium, *PLoS ONE* 8. Article ID: e65223. **[Crossref]**

Ali, F., Khan, I. And Sharidan S. (2014). Closed Form Solutions For Unsteady Free Convection flow Of A Second Grade Fuid over an Oscillating Vertical Plate, *PLoS ONE*, 9(2),e85099. **[Crossref]**

Ching-Yang, C. (2009). Soret and Dufour Effects on Natural Convection Heat and Mass Transfer from a Vertical Cone in a Porous Medium. *International Communication of Heat and Mass Transfer*, 36, 1020–1024. **[Crossref]**

Frank Kamenetskii D.A. (1969): Diffusion and Heat Transfer in Chemical Kinetics. –New York: Plenum Press.

Globe S. (1959) Laminar MHD Flow in an Annular Channel. *Physics of Fluids*, 404, **[Crossref]**

Hamza M. M. (2016). Free Convection Slip Flow of an Exothermic Fluid in a Convectively Heated Vertical Channel, *Ain Shams Engineering Journal*, **[Crossref]**

Hamza M. M., Ojemeri G. and Abdulsalam S (2019). Mixed Convection Flow of Viscous Reactive Fluids with Thermal Diffusion and Radial Magnetic Field in a Vertical Porous Annulus. *Computational Mathematics and Modeling*, 30(3). **[Crossref]**

Hamza, M. M, Ojemeri, G. and Ahmad, S. K. (2023a). Insights into an Analytical Simulation of a Natural Convection Flow Controlled by Arrhenius Kinetics in a Microchannel, Heliyon 9(2023), e17628, pp. 1-13. **[Crossref]**

Hamza, M. M., Ojemeri, G. and Ahmad, S. K. (2023b). Theoretical Study of Arrhenius-Controlled Heat Transfer Flow on Natural Convection Affected by an Induced Magnetic Field in a Microchannel, *Engineering Reports, Wiley*, **[Crossref]**.

Javaherdeh, K., Mirzaei, N. M. and Moslemi, M. (2015). Natural Convection Heat and Mass Transfer in MHD Fluid Flow Past a Moving Vertical Plate with Variable Surface Temperature and Concentration in a Porous Medium. *Engineering Science and Technology an International Journal,* 18, 423-431. **[Crossref]**

Jha B K, Chia R. A. and Babatunde A. (2015). Natural Convection Flow in Vertical Concentric Annuli Filled with Porous Materials having Variable Porosity under Radial Magnetic Field: an Exact Solution, *Asian Journal of Mathematics and Computer Research*, 4, 8-17.

Jha B.K, Ahmad K. S, Ajibade A. O. (2011b). Transient Free Convective Flow of Reactive Viscous Fluid in a Vertical Tube. *International Communications in Heat and Mass Transfer,* 54 2880-2888. **[Crossref]**

Jha B. K., Ahmad K. S. and Ajibade A. O. (2011a). Transient Free-Convective Flow of Reactive Viscous Fluid in a Vertical Channel, International Communication in Heat and Mass Transfer, Elsevier, 38, 633-637. **[Crossref]**

Joshi, H. M. (1987). Free Convection Flows in Vertical Annuli with Two Isothermal Boundaries. *International Communications in Heat and Mass Transfer*,14, 657–664. **[Crossref]**

Kaladhar, K., Motsa S. S. and Srinivasacharya D., (2016) Mixed Convection Flow of Couple Stress Fluid in a Vertical Channel with Radiation and Soret Effects. *Journal of Applied Fluid Mechanics,* 9, 43-50. **[Crossref]**

Makinde O. D. (2008) Thermal Criticality in Viscous Reactive Flows through Channels with a Sliding Wall: an Exploitation of the Hermite-Pade Approximation Method. *Journal of Mathematics and Computational Model,* 47, 312–7. **[Crossref]**

Mozayyeni, H. Rahimi, A.B. (2012). Mixed Convection in Cylindrical Annulus with Rotating Outer Cylinder and Constant Magnetic Field with an

Effect in Radial Direction. *Journal of Science Iranica,* 19, 91–105. **[Crossref]**

Muthuraj R, and Srinivas S, (2010) Mixed Convective Heat and Mass Transfer in a Vertical Wavy Channel with Travelling Thermal Waves and Porous Medium. *Journal of Computers and Mathematics with Applications,* 59, 3516-3528. **[Crossref]**

Obalalu, A. M., O. A. Ajala, A. T. Adeosun, A. O. Akindele, O. A. Oladapo and O. A. Olajide, (2021). Significance of Variable Electrical Conductivity on Non-Newtonian Fluid Flow Between Two Vertical Plates in the Coexistence of Arrhenius Energy and Exothermic Chemical Reaction, Partial Differential Equations in Applied Mathematics, 4,100184, 1-9. **[Crossref]**

Ojemeri, G. and Hamza, M. M. (2022): Heat Transfer Analysis of Arrhenius-Controlled Free Convective Hydromagnetic Flow with Heat Generation/Absorption Effect in a Micro-channel. *Alexandria Engineering Journal,* 61, pp. 12797-12811. **[Crossref]**

Ojemeri, G., Onwubuya I. O. and Abdulsalam S. (2019). Effects of Soret and Radial Magnetic Field of a Free Convection Slip Flow in a Viscous Reactive Fluid Towards a Vertical Porous Cylinder. *Continental Journal of Applied Sciences,* 14(1), 25-45 **[Crossref]**.

Ojemeri, G. and Onwubuya, I. O. (2023a). Analysis of Mixed Convection Flow on Arrhenius-Controlled Heat Generating/Absorbing Fluid in a Superhydrophobic Microchannel: A Semi-Analytical Approach, *Dutse Journal of Pure and Applied Sciences,* 9(2a), pp. 344-357. **[Crossref]**

Ojemeri G., Onwubuya, I. O., Shuaibu A., Omokhuale E. and Altine, M. M. (2023b). Arrhenius-Controlled Heat Transfer Fluid Provoked by Porosity Effect through a Vertical Micro-Channel: An Analytical Approach, *Continental Journal of Applied Sciences,* 18 (1), pp. 18 – 40. **[Crossref]**

Osman, H. I., Omar, N. F. M., Vieru, D. and Ismail, Z. (2022). A Study of MHD Free Convection Flow Past an Infinite Inclined Plate. *Journal of Advanced Research in fluid Mechanics and Thermal Sciences*, 92 (1), pp. 18-27. **[Crossref]**

Reddy, M. G. and Reddy, N. B. (2009). Radiation and Mass Transfer Effects on Unsteady MHD Free Convection Flow of an Incompressible Viscous Fluid Past a Moving Vertical Cylinder. *Journal of Applied mathematics and Mechanics,* 6, 96–110.

Sankar, M. Venkatachalappa, M. Shivkumara, I.S. (2006). Effect of a Magnetic Field on Natural Convection in a Vertical Cylindrical Annulus. *International Journal of Engineering Science and Technology,* 44, 1556–1570. **[Crossref]**

Siva, T., Jaangili, S., and Kumbhakar, B., (2021). Heat Transfer Analysis of MHD and Electroosmotic Flow of Non-Newtonian Fluid in a Rotating Microfluidic Channel: an Exact Solution, *Applied Mathematics and Mechanics*, 42(6), pp 1047-1062. **[Crossref]**

Sravanthi C. S. (2014). Soret Effect on a Steady Mixed Convective Heat and Mass Transfer Flow with Induced Magnetic Field. *International Journal of Science, Engineering and Technological Research,*3, 2278-7798.

Srinivasacharya, D. and K. Kaladhar (2013). Soret and Dufour Effects on Free Convection Flow of a Couple Stress Fluid in a Vertical Channel with Chemical Reaction. *Journal of Industrial Chemical Engineering Quantum,* 19, 45–55. **[Crossref]**

Srinivasacharya, D. and Kaladhar, K. (2014). Mixed Convection Flow of Chemically Reacting Couple Stress Fluid in a Vertical Channel with Soret and Dufour Effects. *International Journal for Computational Methods in Engineering Science and Mechanics,* 15, 413–421. **[Crossref]**

Taid, B. K. and Ahmed, N. B. (2022), MHD Free Convection Flow Across an Inclined Porous Plate in the Presence of Heat Source, Soret Effect and Chemical Reaction Affected by Viscous Dissipation Ohmic Heating, *Bio-interface Research in Applied Chemistry*, 12(5) pp. 6280-6296. **[Crossref]**

Vanita, V. and Kumar, A. (2016). Effect of Radial Magnetic Field on Free Convective Flow over Ramped Velocity Moving Vertical Cylinder with Ramped Type Temperature and Concentration. *Journal of Applied Fluid Mechanics*, 9, 2855-2864. **[Crossref]**

Yale I. D., Uchiri A. M. T., Hamza M. M., and Ojemeri G. (2023). Effect of Viscous Dissipation Fluid in a Slit Microchannel with Heated Superhydrophobic Surface, *Dutse Journal of Pure and Applied Sciences*, 9(3b), pp. 290-302.

APPENDIX

All the Constants used During the Analytical Solutions are Defined here:

$$x_1 = e - \frac{1}{2}, x_2 = \frac{1}{4-2s\,\mathrm{Pr}}, x_3 = \frac{1}{(2-s\,\mathrm{Pr})^2}, x_4 = \frac{1}{2-s\,\mathrm{Pr}}, x_5 = \frac{1}{2-sSc}, z_1 = \frac{s+\sqrt{s^2+4M^2}}{2}, z_2 = \frac{-s+\sqrt{s^2+4M^2}}{2}$$

$$k_1 = \frac{2-s\,\mathrm{Pr}}{1-b}, k_2 = -k_1 b, k_3 = \frac{b^2-1}{2(b-1)}, k_4 = \frac{b^2}{2} - k_3 b, k_5 = \frac{x_2}{b-1}\left\{k_4\left(b^2-1\right) + \frac{k_3\left(b^3-1\right)}{3} + \frac{\left(1-b^4\right)}{12}\right\}$$

$$k_6 = x_2\left(k_4 b^2 + \frac{k_3 b^3}{3} - \frac{b^4}{12}\right) - k_5 b, k_7 = \frac{1}{b-1}\Bigg[x_2\left\{x_2\left(\frac{b^6-1}{360}\right) + k_3\left(\frac{1-b^5}{60}\right) + k_4\left(\frac{1-b^4}{12}\right) +$$

$$\frac{k_5\left(b^3-1\right)}{6} + \frac{k_6\left(b^2-1\right)}{2}\right\} + x_1 x_3\left(\frac{1-b^6}{30} + \frac{k_3\left(b^5-1\right)}{5} + \frac{k_4\left(b^4-1\right)}{3} + \frac{k_3^2\left(1-b^4\right)}{3} + \frac{4k_3 k_4\left(1-b^3\right)}{3} + 2k_4^2\left(1-b^2\right)\right)\Bigg]$$

$$k_8 = \Bigg[x_2\left\{x_2\left(\frac{b^6}{360}\right) - k_3\frac{b^5}{60} - k_4\frac{b^4}{12} +$$

$$\frac{k_5 b^3}{6} + \frac{k_6 b^2}{2}\right\} - x_1 x_3\left(\frac{b^6}{30} - \frac{k_3 b^5}{5} - \frac{k_4 b^4}{3} + \frac{k_3^2 b^4}{3} + \frac{4k_3 k_4 b^3}{3} + 2k_4^2 b^2\right) - k_7 b\Bigg]$$

$$k_9 = \frac{Sr}{b-1}\left\{x_4 k_1\left(1 + b\log b - b\right)\right\} - \frac{2+sSc}{b-1}, k_{10} = Sr\left\{x_4 k_1\left(1 + b\log b - b\right)\right\} - k_9 b$$

$$k_{11} = \frac{Sr}{2-sSc}\left\{2x_2 k_3\left(1 + b\log b - b\right) + 2x_2\left(1-b^2\right)\right\}, k_{12} = Sr\left\{2x_2 k_3\left(1 + b\log b - b\right) + 2x_2\left(1-b^2\right)\right\} - k_{11} b$$

$$k_{13} = \frac{Sr}{b-1}\left[x_4 x_2\left(\frac{b^4-1}{9} + \frac{k_3\left(1-b^3\right)}{2} + 2k_4\left(1-b^2\right) + x_4 k_5\left(1 + b\log b - b\right)\right)\right]$$

$$k_{14} = Sr\left[x_4 x_2\left(\frac{b^4}{9} + \frac{k_3 b^3}{2} + 2k_4 b^2 + x_4 k_5\left(b\log b - b\right)\right)\right] - k_{13}$$

$$k_{15} = \frac{Sr}{b-1}\Bigg[x_4^2\left\{x_2\left(\frac{k_4\left(1-b^4\right)}{9} + \frac{5k_3\left(1-b^5\right)}{48} + \frac{b^6-1}{300}\right) - k_5\frac{\left(1-b^3\right)}{6} - k_6\left(1-b^2\right)\right.$$

$$x_1 x_3 x_4\left(\frac{1-b^6}{50} + \frac{k_3\left(b^5-1\right)}{4} + \frac{4k_4\left(b^4-1\right)}{9} + \frac{4k_3^2\left(1-b^4\right)}{9} + 2k_3 k_4\left(1-b^3\right) + 4k_4^2\left(1-b^2\right)\right)$$

$$\left. x_4 k_7(1 + b\log b - b)\right\}\Bigg]$$

$$k_{16} = Sr\Bigg[x_4^2\left\{x_2\left(\frac{k_4 b^4}{9} + \frac{5k_3 b^5}{48} - \frac{b^6}{300}\right) - k_5\frac{b^3}{4} - k_6 b^2\right.$$

$$x_1 x_3 x_4\left(\frac{2b^6}{50} - \frac{k_3 b^5}{4} - \frac{4k_4\left(b^4\right)}{9} + \frac{4k_3^2\left(b^4\right)}{9} + 2k_3 k_4\left(b^3\right) + 4k_4^2\left(b^2\right)\right)$$

$$\left. x_4 k_7(1 + b\log b - b)\right\}\Bigg] - k_{15} b$$

$$\eta_8 = -2x_2k_4, \eta_{12} = -Nx_5k_{12}, \eta_{15} = x_2x_4k_4, \eta_{16} = -x_4k_5, \eta_{17} = -x_4k_6, \eta_{20} = -NSrx_2x_4x_5k_4, \eta_{24} = -NSrx_4x_5k_5$$

$$\eta_{25} = -Nx_5k_{13}, \eta_{26} = -Nx_5k_{14}, \eta_{27} = \frac{-x_4^2x_2k_4}{12}, \eta_{30} = \frac{-x_4^2k_5}{12}, \eta_{31} = \frac{-x_4^2k_6}{2}, \eta_{32} = x_1x_3x_4, \eta_{35} = \frac{-\eta_{32}k_4}{3}, \eta_{36} = \frac{\eta_{32}k_3^2}{3}$$

$$\eta_{37} = \frac{-4\eta_{32}k_3k_4}{3}, \eta_{38} = 2\eta_{32}k_4^2, \eta_{39} = -x_4k_7, \eta_{40} = -x_4k_8, \eta_{41} = \frac{-NSrx_4^2x_2x_5k_4}{12}, \eta_{44} = \frac{-NSrx_5x_4^2k_5}{6}, \eta_{45} = \frac{-NSrx_5x_4^2k_6}{2}$$

$$\eta_{48} = N\eta_{35}Srx_5, \eta_{49} = N\eta_{36}Srx_5, \eta_{50} = N\eta_{37}Srx_5, \eta_{51} = N\eta_{38}Srx_5, \eta_{52} = \frac{-NSrx_4^2x_2x_5k_4}{36}, \eta_{55} = \frac{-NSrx_4^2x_5k_5}{12},$$

$$\eta_{56} = \frac{-NSrx_4^2x_5k_6}{2}, \eta_{60} = \frac{N\eta_{32}Srx_5k_3^2}{9}, \eta_{61} = \frac{2NSrx_5k_3k_4}{2}, \eta_{62} = 2\eta_{32}NSrx_5k_4^2, \eta_{63} = NSrx_5x_4k_7\left(\log(r) - r\right)$$

$$\eta_{64} = -Nx_5k_{15}, \eta_{65} = -Nx_5k_{16}$$

$$B_3 = \frac{\eta_8 + \eta_{12}}{2 + 2(1-s) - M^2}, B_7 = \frac{\eta_{15} + 2\eta_{20}}{12 + 4(1-s) - M^2}, B_8 = \frac{\eta_{16} + \eta_{24} + \eta_{25}}{6 + 3(1-s) - M^2}$$

$$B_9 = \frac{\eta_{16} + \eta_{26}}{2 + 2(1-s) - M^2}, B_{13} = \frac{\eta_{27} + \eta_{35} + \eta_{36} + \eta_{41} + \eta_{48} + \eta_{49} + \eta_{52} + \eta_{60}}{30 + 6(1-s) - M^2}$$

$$B_{14} = \frac{\eta_{30} + \eta_{37} + \eta_{44} + \eta_{50} + \eta_{55} + \eta_{61}}{20 + 5(1-s) - M^2}, B_{15} = \frac{\eta_{31} + \eta_{38} + \eta_{45} + \eta_{51} + \eta_{56} + \eta_{62}}{12 + 4(1-s) - M^2}$$

$$B_{16} = \frac{\eta_{39} + \eta_{63} + \eta_{64}}{6 + 3(1-s) - M^2}, B_{17} = \frac{\eta_{40} + \eta_{65}}{2 + 2(1-s) - M^2}, A_3 = -\left(A_4 + B_3\right),$$

$$A_4 = \frac{B_3}{b^{z1} - b^{-z2}}\left(b^2 + b^{z1}\right), A_5 = -(A_6 + B_7 + B_8 + B_9),$$

$$A_6 = \frac{1}{b^{z1} - b^{-z2}}\left\{B_7\left(b^4 - b^{z1}\right) + B_8\left(b^3 - b^{z1}\right) + B_9\left(b^2 - b^{z1}\right)\right\},$$

$$A_7 = -(A_8 + B_{13} + B_{14} + B_{15} + B_{16} + B_{17}), A_8 = \frac{1}{b^{z1} - b^{-z2}}\left\{B_{13}\left(b^6 - b^{z1}\right) + B_{14}\left(b^5 - b^{z1}\right) + B_{15}\left(b^4 - b^{z1}\right)\right.$$

$$\left. B_{16}\left(b^3 - b^{z1}\right) + B_{17}\left(b^2 - b^{z1}\right)\right\}$$